Journal of the European Ceramic Society **12** (1993) 323–336

State of the Art

Structural Integrity of Ceramic Multilayer Capacitor Materials and Ceramic Multilayer Capacitors

G. de With*

Philips Research Laboratories, PO Box 80000, 5600 JA, Eindhoven, The Netherlands

(Received 10 March 1993; accepted 3 June 1993)

Abstract

An overview is given of the fracture of and stress situation in ceramic capacitor materials and ceramic multilayer capacitors. A brief introduction to the relevant concepts is given first. Next the data for capacitor materials and the data for capacitors are discussed. It is shown that the materials data are not directly transferable to the components. A wide variability of component properties exist, dependent on all microstructural features. Details on the microstructure itself are generally lacking. It is concluded that the effect and amount of subcritical crack growth and residual stress in the ceramic and of relaxation of the metal parts on the mechanical behaviour of capacitors is insufficiently known for reliable longevity predictions.

Es wird eine Übersicht über das Bruchverhalten von und den Spannungszustand in Keramik- und Mehrschichtkeramikkondensatoren gegeben. Zunächst folgt eine kurze Erläuterung einiger wichtiger Vorstellungen. Anschließend werden die Daten der Kondensatormaterialien und der Kondensatoren diskutiert. Es wird gezeigt, daß sich die Daten der Materialien nicht direkt auf die Komponenten übertragen lassen. Abhängig vom Mikrogefüge besitzen die Komponenten sehr unterschiedliche Eigenschaften, wobei in den meisten Fällen keine detaillierten Informationen über das Mikrogefüge vorliegen. Es läßt sich schließen, daß der Effekt und das Ausmaß des unterkritischen Rißwachstums und der Restspannung in der Keramik, sowie die Relaxation der Metallkomponenten auf das mechanische Verhalten von Kondensatoren nicht in ausreichendem Maße bekannt ist, um die Lebensdauer zuverlässig vorherzubestimmen.

Cet article présente une vue d'ensemble des phénomènes de fracture et des états de contrainte dans les condensateurs en céramique, ou composés de multicouches céramiques. En premier lieu, on introduit les concepts appropriés à ce problème. Puis les données existantes sur les matériaux pour condensateurs, et sur les condensateurs eux-mêmes, sont discutées. On montre que les données sur les composants ne se déduisent pas directement des données sur les matériaux qui les composent. Les propriétés des composants sont très variables; elles dépendent de toutes leurs caractéristiques microstructurales. En général, des détails sur cette microstructure manquent. On conclut que les effets mécaniques et l'importance de la croissance sous critique de fissures et des contraintes résiduelles dans la céramique, d'une part, d'autre part du relâchement des contraintes dans le métal sont trop mal connus pour permettre des prédictions fiables sur la tenue de ces condensateurs.

1 Introduction

In spite of the fact that ceramic multilayer capacitors (CMCs) form worldwide a substantial business, the available information on the mechanical properties of the materials involved and components themselves is limited. Also the data on stresses in the mounted CMCs available in the literature are limited. For the assessment of the structural integrity of CMCs, information on the mechanical properties of the materials involved and the stress distribution is a prerequisite.

Most of the present ceramics used for CMCs are titanate based. A brief introduction to titanate materials is given in Section 3.1, while the same is done for CMCs in Section 4.1. For a general outline of the manufacturing process of CMCs reference is made to the literature: the detailed overview by Kahn *et al.*[1] or the much shorter paper by Hennings.[2] A schematic view of a CMC is given in Fig. 1. For proper understanding of this paper, it should be noted that the Electric Industries Associ-

* Also affiliated to the Centre for Technical Ceramics, Eindhoven University of Technology, PO Box 513, 5600 MD, Eindhoven, The Netherlands.

Journal of the European Ceramic Society 0955-2219/93/$6.00

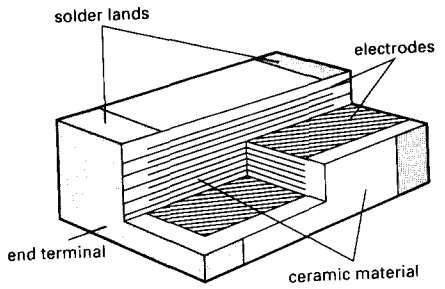

Fig. 1. A cutaway view of a CMC showing the internal electrodes and end terminations.

ation (EIA) has standard indications for size (width and length in units of 0·01 inch) and types (abbreviations like X7R, Z5U, etc.). The field of structural integrity of CMCs can be divided into three parts: related to materials processing, related to components testing and related to board processing. In this paper primarily the information available in the literature on the mechanical aspects related to materials processing of CMC materials and CMCs is reviewed. However, in this introduction, a few words will be said about components testing and board processing.

Components testing can be done in many ways. A few are mentioned below, not all yet commonly implemented:

—Visual testing.
—Insulation resistance testing.[3]
—Highly accelerated life testing.[4]
—Electromechanical testing.[5]
—Acoustic emission testing.[6,7]
—Scanning laser acoustic microscopy.[8]
—Acoustic attenuation testing.[9]
—Thermal shock testing.[10–16]

Many of these techniques do discriminate reasonably well between 'bad' and 'good' capacitors. The problem usually is the definition of 'good' and 'bad'.

Components processing is capable of introducing severe damage into the CMCs. Here only three aspects are referred to. Firstly, there is the pick-and-place procedure, necessary for positioning the components on the circuit board. This procedure may be accompanied by highly localized Hertzian stresses and therefore introduces (micro)cracks resulting in a low(er) strength. Secondly, there is the soldering procedure, necessary for mounting the components on the circuit board. This procedure may be the origin of thermal shock failure. Thirdly, there is the bending of boards which often occurs during further processing. Bending occurs during 'unwarping', opposite site mounting, board depanelization, testing, connector and component assembling. The accompanying stress may result in fracture of a component. A good overview of the possible problems in this area is given by Maxwell.[17]

As mentioned, this paper focuses on the materials aspects of the structural integrity. In Section 2 a brief discussion on the fracture behaviour of brittle materials is given. The materials properties are discussed in Section 3, while Section 4 deals with the CMC behaviour. In Section 5 the effect of residual stress is discussed. Finally, in Section 6 some general conclusions are presented.

2 Aspects of Brittle Failure

In this section some aspects of brittle failure are briefly described. This is mainly done to set the notation. For a more complete discussion reference is made to the literature.[18,19]

In a ceramic material flaws are generally present. These flaws are usually microcracks, pores, etc. When a (uniaxial) tensile stress is applied, a stress concentration occurs at these flaws. This stress concentration is quantified by the stress intensity factor, K_I, given by

$$K_I = (Y/Z)\sigma\sqrt{a}$$

where Y is a geometrical factor dependent on loading conditions, Z is a geometrical factor dependent on the shape of the flaw, σ is the applied stress and a denotes the size of the flaw. Catastrophic failure occurs, roughly speaking, when the stress at the flaw tip exceeds the theoretical strength. The corresponding critical stress intensity factor, K_{Ic}, is usually called fracture toughness. The strength, σ_f, is related to K_{Ic} and the size of the critical flaw, a_c, by

$$K_{Ic} = (Y/Z)\sigma_f\sqrt{a_c}$$

Typical values for the fracture toughness of ceramics are between 0·5 and 4·0 MPa $m^{1/2}$. The fracture toughness is directly related to the fracture energy, J_f, the amount of energy necessary for creating a unit area of fracture surface. For linear elastic materials loaded in plane strain this relation reads

$$J_f = (1 - \nu^2)K_{Ic}^2/2E$$

where ν is Poisson's ratio and E is Young's modulus. Typical values are a few to a few tens J/m^2. Combining these equations yields

$$\sigma_f = (Z/Y)[2J_fE/(1 - \nu^2)a_c]^{1/2}$$

Strength is thus a hybrid quantity, on the one hand dependent on the intrinsic (material) properties J_f, E and ν, and on the other hand on the extrinsic (processing-dependent) defect size a_c. The distribution of strength, that is in essence the flaw size distribution, is often described by so-called weakest-link statistics. The failure probability, P_f, is the essential quantity and is given by

$$P_f = 1 - \exp[-(\sigma_f/\sigma_o)^m]$$

The parameter m is called the Weibull modulus and describes the width of the distribution. Typical values are between 5 and 25. The parameter σ_0 describes the location of the strength distribution and is dependent on the size of the specimen and the stress distribution. When $\sigma_f = \sigma_0$, $P_f = 0{\cdot}63$. The characteristic strength σ_0 is related to the mean strength, $\bar{\sigma}$, as measured in a set of strength measurements, by $\bar{\sigma} = (1/m)!\sigma_0$.

Three more complications arise. Firstly, there is the case of biaxial or other stress situations. The translation of uniaxial strength data into biaxial data is not unequivocally clear. The biaxial strength may be lower or higher than the uniaxial strength. Apart from the Weibull modulus m, the exact factor depends on the choice of equivalent stress. An experimentally validated, generally applicable equivalent stress, like von Mises stress for metals, does not exist for ceramics. Secondly, highly relevant for CMC materials and CMCs is residual stress, here denoted by σ_r. These stresses should be taken into account in the fracture equation. That means that the applied stress, σ, should be replaced by an effective stress, σ_e, given by

$$\sigma_e = \sigma + \langle \sigma_r \rangle$$

where $\langle\ \rangle$ denotes a proper average over the residual stress. Compressive residual stress increases the observed strength, while tensile stress decreases the observed strength. Thirdly, at K_I values less than K_{Ic} also subcritical crack growth (SCG) occurs. The rate of crack propagation is often described phenomenologically by

$$\dot{a} = \dot{a}_0 (K_I / K_{Ic})^n$$

where $\dot{a}_0$ and n are the SCG parameters. The higher the value of n, the less susceptible the material is to slow crack growth. Typical values range from $n = 15$ to 40. An initially subcritical flaw of size a_i thus increases with time until failure occurs at $a = a_c$. Failure time, t_f, is an important quantity given by

$$t_f = \int_{a_i}^{a_c} (1/\dot{a})\, \mathrm{d}a$$

and thus depends on a_i, K_{Ic}, σ, $\dot{a}_0$ and n. It should be clear by now that fracture of materials is a complex phenomenon.

Finally it should be noted that the description of fracture behaviour along the lines indicated above, neglects coupling between mechanical and piezo-electrical phenomena. This coupling is obviously present and has recently been addressed by Suo *et al.*[20] from a theoretical point of view. The limited experimental data present[21,22] indicate, however, a limited effect so far.

3 Capacitor Materials

3.1 Brief introduction to titanate materials

Frequently CMC materials are based upon $BaTiO_3$. Many titanates have the perovskite structure. Titanates show a phase transformation at the Curie temperature, T_C, for pure $BaTiO_3$ at about 125 °C. Above this temperature the material is cubic and paraelectric (PE). Below this temperature the material is tetragonal and ferroelectric (FE). In almost all cases substitutions are made (e.g. Ba partially replaced by Ca, etc.) to control the Curie temperature. Also additives are used which modify the dielectric and electric behaviour. The dielectric permittivity versus temperature is highly dependent on the microstructure, that is, main composition, second phases and grain size (distribution) of the material. It is probably superfluous to state that these materials have been largely optimized with respect to their functional behaviour without considering their structural behaviour. Finally, it is important to note that the tetragonal and cubic phases have different thermo-physical properties, e.g. thermal expansion coefficient, specific volume and elastic constants.

3.2 Material mechanical properties

In this section the mechanical properties of the ceramics as such are discussed. Toughness, strength and sub-critical crack growth will be dealt with in turn.

3.2.1 Toughness

The fracture toughness is in principle a material property. To put this statement into perspective, two important remarks should first be made.

The first remark deals with the experimental technique used. The values of the fracture toughness reported in the literature are measured in various ways. One can distinguish between methods using microcracks (using primarily indentation methods) and macrocracks (using specimens like three-point bend and double cantilever beam). While the former have the advantage that they deal with a crack of similar size as occurs in practice, they have also the disadvantage that the influence of residual stress due to crystal anisotropy, surface effects and or the indentation itself is quite pronounced. Often therefore there are large discrepancies between data from microcrack and macrocrack methods.

The second remark deals with the materials. Only in rare circumstances is sufficient information presented on the microstructure of the materials involved. That means that details on composition, grain size (distribution), second phases, porosity, etc., are not provided, which makes a proper comparison

Table 1. Fracture energy data at room temperature (ferroelectric state)

Material	ρ_r	d (μm)	J_f (J/m^2)	K_{Ic} ($MPa\,m^{1/2}$)	*Method*	*Refs*
BT pure, HP, A, S	~0·99	1·5	2·9	(0·84)	DCB	27
BT pure, HP, A, S	~0·99	150	7·5	(1·37)	DCB	27
BT LiF + MgO, HP, A	0·99	Bimodal	6·2	(1·25)	DCB	27
BT C, A, S	0·96	20	3·8	(0·97)	DCB	27
BT C, S	0·95	5	4·5	(1·06)	DCB	27
RE, NPO	—	1–3	(7·8)	1·4	I–σ	25
BT, X7R	—	<1	(2·0)	0·7	I–σ	25
BT, Bi, X7R	—	<1	(4·8)	1·1	I–σ	25
BT, Z5U (low aging)	—	3–7	(3·2)	0·9	I–σ	25
BT, Z5U (high aging)	—	3–7	(4·8)	1·1	I–σ	25
BT Z5U	—	3–7	(2·0)	0·7	I–σ	25
BT, X7R	—	<1	(2·0)	0·7	I–σ	25
BT	—	7	(3·2)	0·86	I–σ	30
BT	0·97	—	(3·7)	0·96	I–σ	30
BT, X7R, Bi	—	—	(9·0)	1·5	I–σ	30
ANPO Nd doped, ⊥	—	—	(6·8)	1·30	AM-DCB	38
ABX Ta doped, ⊥	—	—	(2·1)	0·72	AM-DCB	38
K2300	—	—	(2·6)	0·80	DCB	37
K2300	—	—	(3·7)	0·96	DCB-TC	37
K2300, ⊥	—	—	(3·3)	0·91	DT	37
K2300, //	—	—	(2·5)	0·79	DT	37
K2300	—	—	(2·9)	0·85	I–a	37
Various	—	—	(10·1)	1·64	I–a	37
COG	—	—	(4·6)	1·07	I–σ	39
X7R	—	—	(2·6)	0·81	I–σ	39
Z5U	—	—	(2·6)	0·81	I–σ	39

d: Grain size; ρ_r: relative density; J_f: fracture energy; K_{Ic}: fracture toughness; BT: $BaTiO_3$; RE: rare earth; HP: hot-pressed; A: annealed; S: semi-polished; C: commercial; DCB: double cantilever beam; AM: applied moment; TC: thermally cracked; DT: double torsion; I–σ: indentation and strength; I–a: indentation and crack length; ⊥: fracture plane perpendicular to (imaginary) electrode plane; //: fracture plane parallel to (imaginary) electrode plane. All data as given in the reference (no parentheses) and as calculated from the fracture toughness or energy (in parentheses) assuming $E = 125$ GPa and neglecting ν. NPO, X7R, etc., denote various material specifications according to the EIA specification. K2300 represents a material with permittivity 2300.

of the various data difficult. A similar situation exists for high T_C superconductors.

In Table 1 fracture energy data below T_C as collected from the literature are presented. In this table for each set of materials J_f and K_{Ic} data are given together with an average value for the microstructural data (density, grain size), as far as can be distilled from the original data. Many publications on the fracture behaviour of titanates are due to Pohanka, Freiman and coworkers.[21–30] However, the overlap between the various publications is considerable. The information from other sources is generally not of a systematic nature. The value of J_f for small grain size below T_C is approximately 2–5 J/m^2, corresponding to a fracture toughness of about 0·7–1·0 MPa m$^{1/2}$, assuming a Young's modulus of 125 GPa. For larger grain size, larger values of fracture energy are observed, up to 10 J/m^2.

In Table 2 fracture energy data above T_C are given. Above T_C values ranging from 3–4 J/m^2 are generally observed, but independent of the grain size. The value of the fracture toughness below the Curie temperature, is thus somewhat higher than above T_C. The increase is attributed to the presence of ferroelectric 90° domains which increase the roughness of the fracture surface. A similar increase has also been observed for thermistor ceramics.[31]

Table 2. Fracture energy data at elevated temperature (paraelectric state)

Material	ρ_r	d (μm)	J_f (J/m^2)	K_{Ic} ($MPa\,m^{1/2}$)	*Method*	*Refs*
BT pure, HP, A, S	~0·99	1·5	2·5	(0·78)	DCB	27
BT pure, HP, A, S	~0·99	150	3·0	(0·87)	DCB	27
BT LiF + MgO, HP, A	0·99	Bimodal	3·2	(0·89)	DCB	27
BT C, A, S	0·96	20	2·5	(0·78)	DCB	27
BT C, S	0·95	5	4·3	(1·04)	DCB	27
BT	—	7	(9·0)	1·5	I–σ	29

For an explanation of abbreviations and symbols, see Table 1.

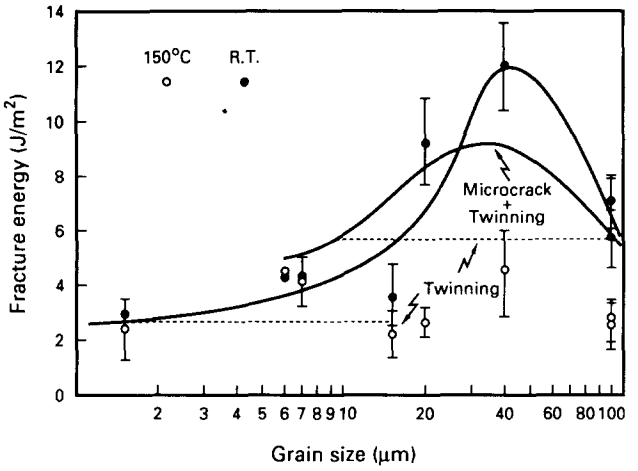

Fig. 2. The fracture energy of nominally pure $BaTiO_3$ at room temperature and 150 C as a function of grain size. While the room temperature data show a peak at about 40 μm, the 150 C data are independent of grain size. Data according to Pohanka *et al.*[22] The dashed line is the prediction according to the model as discussed by the same authors.

From the data in Tables 1 and 2 it also becomes evident that there is no clear relation between composition and toughness.

The behaviour of the fracture energy of nominally pure $BaTiO_3$ as a function of grain size is given in Fig. 2. A maximum of about 10 J/m^2 is observed for a grain size of about 40 μm. This maximum is due to a trade-off between enhanced energy dissipation by microcracking/twinning and microcrack linking. Pohanka *et al.*[22] also propose a semi-quantitative model for this behaviour. Taking reasonable values for the parameters involved results in an acceptable correspondence with the experimental data. For application in X7R capacitors, one is interested in the small grain size region with the value of around 3 J/m^2.

Pohanka *et al.* emphasized the importance of internal stress. Due to the anisotropy of the tetragonal material, internal stresses arise at mechanical defects. If the flaw size is large as compared with the grain size, the effect of these stresses

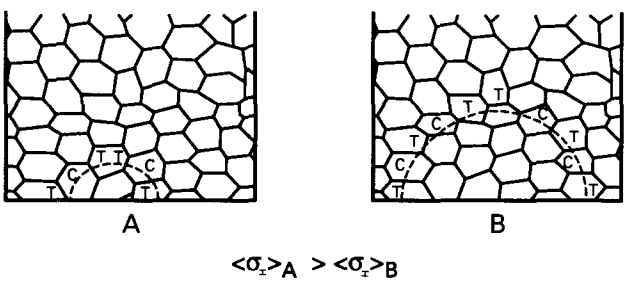

Fig. 3. Schematic of the averaging of the internal stress. The flaw is schematically indicated with the dashed line. The T and C denote grains with tensile and compressive stress respectively. For A the flaw size is comparable to the grain size, resulting in a non-zero effective internal stress over the flaw. For B the flaw size is much larger than the grain size, resulting in a zero effective internal stress over the flaw. This results in lower strength for situation A in case of a tensile effective internal stress. According to Pohanka *et al.*[28]

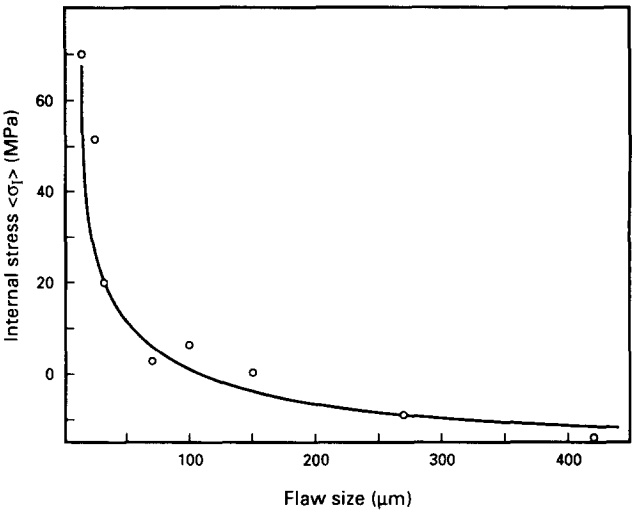

Fig. 4. Internal stress as a function of flaw size for $BaTiO_3$ ceramics as determined from fracture energy considerations. According to Pohanka *et al.*[28]

averages to zero (Fig. 3). If the flaw size is comparable to the grain size, a non-zero effective internal stress $\langle\sigma_i\rangle$ over the flaw results. Solving the fracture equation for the paraelectric and ferroelectric state for $\langle\sigma_i\rangle$, assuming equivalent values for Young's modulus E and flaw size a, results in

$$\langle\sigma_i\rangle = \sigma_f(\mathrm{PE})[J_f(\mathrm{FE})/J_f(\mathrm{PE})]^{1/2} - \sigma_f(\mathrm{FE})$$

The amount of internal stress as determined by these authors[21] in this way is given in Fig. 4. The order of magnitude of the internal stress is comparable as can be calculated from dielectric (domain) models.[32,33] Clearly the effect of internal stress is considerable.

In some papers high values of fracture toughness (2·2–3·4 MPa m$^{1/2}$) have been reported, e.g. Ref. 34 These data result invariably from estimates based on crack length as a result of indentation tests. The effect of compressive residual stress is usually neglected.

The materials investigated can be divided roughly into relatively pure barium titanate and modified titanates. All data observed for pure $BaTiO_3$ are reasonably consistent. For the modified materials the value of the toughness is largely dependent on the exact composition, grain size, etc. Here the influence of the microstructure is thus evident though a clear trend is not present.

One could expect that anisotropy would play an important role. No significant amount of information has been found with regard to this aspect for titanates. However, some information is available for lead zirconate titanate type materials.[35,36] For these materials a ratio up to about 3 is obtained for fracture energies for fracture planes perpendicular and parallel to the preferred axis. For $BaTiO_3$ only a slight effect (0·92 versus 0·79 MPa m$^{1/2}$) has been observed.[37] Finally one could expect that, since barium titanate is also piezoelectric, poling the

material influences the value of the fracture toughness. From experiments done so far[21,22] the influence of poling has been assessed as negligible. The effect of an applied electric field is assessed differently by different authors. According to one author[30] the field retards crack growth slightly for a crack plane orientation perpendicular to the field and has no effect for a parallel orientation. According to another,[37] no effect can be detected up to at least 10 kV/cm.

3.2.2 Strength

Ceramic capacitors are mounted by soldering and tested by bending the circuit board in various fashions. For the latter data on strength at room temperature are important. Since the soldering procedure uses temperatures generally far above the Curie temperature, the strength at these temperatures is also important. In Table 3 the strength data from the literature are collected. Strength values between 100 and 150 MPa are generally observed, though some considerably higher values are reported as well. It is reported by Freiman, Pohanka and coworkers that the strength above the Curie temperature is higher than below T_C. This is due to the absence of the internal stress above T_C. The decrease in K_{Ic} is clearly more than compensated.

However, Cook *et al.*[29] reported a decrease in strength for indented specimens as a function of temperature (25°C to 170°C). The reason for the discrepancy between these observations is unknown.

Although not always clearly stated, the materials as discussed by Freiman, Pohanka and coworkers are used in an annealed state, typically 10–30 h at 900–1300°C, to obtain various grain sizes. It is assumed that no surface residual stress is present. For machined, modified titanate ceramics, however, it has been shown that a substantial amount of residual stress due to the machining operation is present.[31] This stress is due to the fact that the surface remains to a large extent cubic below T_C, while the tetragonal state at the surface is only reached after considerable temperature rise above T_C. For these materials an anomalous behaviour of strength with respect to fracture toughness was observed. The behaviour was explained by the difference in thermal expansion coefficient and specific volume of the cubic and tetragonal phase. This results in a tensile surface stress above T_C and a compressive surface stress below T_C. Together with the compressive stress due to the machining operation itself, the total surface residual stress is compressive below the Curie temperature and tensile above the Curie temperature. A lower strength thus results above the Curie temperature.

As for the K_{Ic}, there are just a few anisotropy effects on the strength reported[38] in the literature. It is to be expected that if the monolithic material is fabricated in the same way as the CMC (Doctor Blade sheet pressed together with considerable pressure at slightly elevated temperature), the material will be anisotropic. Indeed a slight anisotropy of about 5–10 MPa on the overall strength of 100–250 MPa has been reported.

The variation in strength as indicated by the Weibull modulus is described only a few times[39] Typically Weibull moduli in the range of 3 to 6 are reported for the as-fired materials. A treatment in a 'corner rounding' apparatus increased the m value initially to about 10–13, but a decrease to about 7 follows at longer treatment times. Koripella[39] also reports that the theoretical critical temperature difference for thermal shock corresponds well with the experimental value. For X7R materials an allowed temperature difference of about 125°C was estimated.

A correlation between dielectric breakdown and mechanical breakdown has been observed by Yanagida and coworkers.[40–42] An example of this correlation is shown in Fig. 5. Although the

Table 3. Strength data

Material	ρ_r	d (μm)	σ_f (*FE*) (*MPa*)	σ_f (*PE*) (*MPa*)	*Method*	*Refs*
BT pure, HP, A, S	~0·99	1·5	115	190	3-pb	23
BT pure, HP, A, S	~0·99	150	90	155	3-pb	23
BT LiF + MgO, HP, A	0·99	Bimodal	160	170	3-pb	23
BT C, A, S	0·96	20	90	155	3-pb	23
BT C, S	0·95	5	130	135	3-pb	23
ANPO Nd, ⊥	—	—	252	—	3-pb	38
ANPO Nd, //	—	—	241	—	3-pb	38
ABX Ta, ⊥	—	—	110	—	3-pb	38
ABX Ta, //	—	—	105	—	3-pb	38
K2300	—	—	76–106[a]	—	4-pb	37
COG	—	—	198	—	3-pb	39
X7R	—	—	168	—	3-pb	39
Z5U	—	—	114	—	3-pb	39

3(4)-pb: Three (four)-point bend; for an explanation of the other abbreviations and symbols, see Table 1.
[a] Dependent on stress rate.

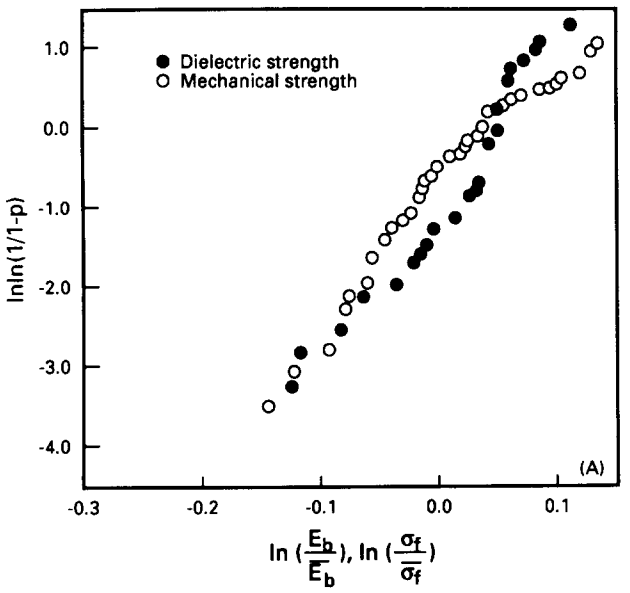

Fig. 5. Correspondence between dielectric and mechanical breakdown. Weibull plot of the mechanical and dielectric strength for a $BaTiO_3 + 0{\cdot}4$ wt% MnO ceramic. According to Yamashita *et al.*[40]

interpretation of this correlation is not clear, the similarity of the Weibull curves suggests that both types of failure occur as a result of the same flaws.

3.2.3 Subcritical crack growth

In Table 4 data on the SCG exponent n have been collected. A wide range of values is observed. The experiment with the largest stress rate range is clearly the one by Freiman, Pohanka and coworkers. This result for pure $BaTiO_3$ has been mentioned several times.[21,25,26,30] The value quoted, $n = 67$, is quite high. It should be recognized that these data were obtained with (indented) biaxial (ball-on-three ball) tests using not entirely flat specimens. Systematic errors in strength can arise with this test, while the slow crack growth behaviour under biaxial stress is also unclear. A fatigue limit was suggested for X7R ('pure') $BaTiO_3$ material.[25] However, the existence of a fatigue limit seems to be doubtful because the suggestion was based on the neglect of one data point. In this case strength was independent of the stress rate. Other researchers never observed this. However, other researchers, admittedly using a smaller stress rate range, quote much lower n values, typically around 30. With such a value in long-term applications of CMCs the effect of SCG should clearly be taken into consideration. The origin of these discrepancies can probably be found in the different microstructures and measuring procedures. While most of the data of Pohanka, Freiman and coworkers were obtained with indented specimens, other researchers often use machined specimens. The influence of the residual stress on the machined specimens is not known. For indented specimens in the I–$\dot{\sigma}$ experiments (see Table 4), the relation between the n value as measured, n', and the real n value, n, is given by $n = (4n' - 2)/3$.[45] In the case where machined specimens are used, the relation is unknown. Apart from a lack of microstructural data, this is a reason why, unfortunately, the relation of slow critical crack growth to the microstructure of the various materials is not clear. Perhaps it can be concluded that a higher value results for purer materials and for smaller grain size.

4 Capacitors

4.1 Brief introduction to capacitors

A schematic view of a CMC is given in Fig. 1. This component is constructed from alternating layers of dielectric ceramic and metal electrodes. As mentioned already, the dielectric ceramic is usually

Table 4. SCG parameters

Material	*n*	*d* (μm)	ρ_r	*Method*	*Refs*
X7R	158	<1		I–$\dot{\sigma}$	25
X7R Bi	85	<1	—	I–$\dot{\sigma}$	25
Pure BT	67	7	>0·99	I–$\dot{\sigma}$, 6 D, water	21, 25, 26, 30
Industrial grade	33	5	0·94	—	22
Z5U	58	3–7		I–$\dot{\sigma}$, 6 D, water	25
RE NPO	99	1–3		I–$\dot{\sigma}$, ?	25
Z5U BT	58	3–7		I–$\dot{\sigma}$, ?	25
K2300	22	—	—	I–$\dot{\sigma}$, 3 D, 30% RH	37
Pure BT	33			I–$\dot{\sigma}$, ?	37
Z5U	~17			DT, water	43
Z5U	~27		—	DT, air	43
Z5U	>100	—		DT, toluene	43
Z5U	35	—		σ–$\dot{\sigma}$, 1 D	43
Modified	23	4	0·915	σ–$\dot{\sigma}$, 2 D	44
	28	6	0·929	σ–$\dot{\sigma}$	44
	37	5	0·938	σ–$\dot{\sigma}$	44
	38	11	0·949	σ–$\dot{\sigma}$	44

D: Decades in stress rate; σ–$\dot{\sigma}$: strength stress rate; I–$\dot{\sigma}$: indentation stress rate; for an explanation of the other abbreviations and symbols, see Table 1.

Table 5. CMC toughness data

Method	J_f (J/m^2)	K_{Ic} ($MPa\,m^{1/2}$)	*Method*	*Refs*
K1500, //	(3·2)	0·89	AM-DCB	38
K1500, ⊥	(5·7)	1·19	AM-DCB	38
K2300, //	(5·0)	1·12	AM-DCB	38
K2300, ⊥	(8·5)	1·46	AM-DCB	38
BX K2000	—	0·9–1·7	*I*	37
COG	(9·0)	1·5	*I–σ*	39
X7R	(4·2)	1·03	*I–σ*	39
Z5U	(4·1)	1·01	*I–σ*	39
BX	—	1·1–1·3	*I–σ*	46 Unidentified samples
K2300	—	0·85–1·7	*I–σ*	46 Unidentified samples
K60	—	1·5–2·2	*I–σ*	46 Unidentified samples

For an explanation of abbreviations and symbols, see Table 1.

perovskite based. An important trend for increasing the capacitance per unit volume is to decrease the dielectric thickness. For high-quality CMC the electrodes are frequently based on noble metal alloys, notably Pd and Ag. The end terminations are required for both the connection of the various electrodes and the soldering later on. They are usually made from a glass–metal composite paste and sometimes provided with a Ni coating.

The production process of a CMC is roughly as follows. A foil is cast using the Doctor Blade technique and after drying the electrode paste is sieve printed on the foil. Next the separate foils are stacked together properly and laminated, e.g. pressed at slightly elevated temperature. After separating the individual CMCs from these plates, the binder is burned out and sintering takes place. After corner rounding the end terminations are provided.

4.2 Component mechanical properties

In this section the fracture toughness, strength, subcritical crack growth and defects in CMCs will be discussed.

4.2.1 Toughness

Data as gathered for CMCs are given in Table 5. From these data two things become clear. The value of K_{Ic} is generally slightly larger than for monolithic materials and the value for K_{Ic} is anisotropic.

Firstly, consider the overall value of K_{Ic}. One would expect a higher value of CMCs than for the materials because of the ductility of the metal electrodes. Indeed most papers report an increase.[37–39] The increase is, however, limited to a few tens of a percent.

Secondly, consider the anisotropy. The fracture resistance for a fracture plane perpendicular to the electrodes is typically 30% higher than for a plane parallel to the electrodes. The crack has to extend through the metal electrode, thereby dissipating energy during the plastic deformation. For the experiments discussed a macroscopic toughness test was used. It should be kept in mind, however, that many data have been collected by indentation technique which is even more influenced by the residual stresses in the CMC.

In some papers, e.g. Refs 37 and 46, fracture toughness data are presented for commercially available CMCs with no further information on microstructure. Only the order of magnitude has been included in Table 5.

Investigations by Vickers indentation on various places on the CMCs have been carried out.[47,48] From these investigations it appears that a higher toughness is present between or at the electrodes. While the latter can easily be rationalized by ductility arguments, the former is related to the residual stress. A compressive stress, due to the difference in thermal expansion coefficient between the metal electrode and ceramic dielectric, is present between the electrodes. This compressive stress retards the crack propagation. These types of measurements in fact do not represent the material's properties *per se*, but the material's properties combined with (macroscopic and microscopic) residual stress. It has been suggested that indentation can be used as a quality assessment method.[48] Indeed, differences between two batches were detected, although it is not made clear at all whether this represents typical or extreme differences.

4.2.2 Strength

The availability of strength data in the open literature is again limited. Data have been collected in Table 6. The overall value of the strength ranges from 90 to 280 MPa. Smaller size results in a higher strength. The strength is generally measured by a three-point test. Not too much value should be given to the exact numerical values, in view of the experimental difficulties with the small specimen size. Like the fracture toughness, the strength is anisotropic. A higher strength is sometimes observed for a fracture plane perpendicular to the electrodes.

Table 6. CMC strength data

Material	σ_f (*FE*) (*MPa*)	*Method*	*Refs*
K1500, //	150	3-pb	38
K1500, ⊥	150	3-pb	38
K2300, //	208	3-pb	38
K2300, ⊥	168	3-pb	38
COG 5819 size	175	3-pb	39
COG 1206, 0·76 mm	285	3-pb	39
COG 1206, 1·27 mm	218	3-pb	39
X7R 5819 size	166	3-pb	39
X7R 1206, 0·76 mm	254	3-pb	39
X7R 1206, 1·27 mm	215	3-pb	39
Z5U 5819 size	116	3-pb	39
Z5U 1206, 0·76 mm	181	3-pb	39
Z5U 1206, 1·27 mm	143	3-pb	39
BT (electr. diff.)	120–150	3-pb	50
Y5U	90–130	3-pb	50
X7R	125	3-pb	50

For an explanation of abbreviations and symbols, see Table 1.

This is partly due to the anisotropy of K_{Ic}. Also it seems obvious that defects can develop more easily parallel to the electrodes than perpendicular to the electrodes. The limited data on K_{Ic} and σ_f do not substantiate this idea, however. The ratio of parallel and perpendicular strength is similar to the toughness ratio. However, overall correlation between strength and toughness is poor, as could be expected in the presence of varying residual stress. One would expect to see the increased toughness reflected in an increased strength. For small sizes (1206) this is indeed sometimes observed,[39] but others also find the reverse.[38] For larger size (5919) the strength of electroded specimens is less than for non-electroded specimens. This is probably related to increased defects due to a more difficult binder removal procedure.

Some biaxial tests (ball-on-three ball) have been carried out.[38] From these data, which show a wide scatter, the conclusion is drawn that the (biaxial) strength decreases with increasing thickness of the CMCs. The amount of shear stress is, however, also increased with increasing thickness and therefore this conclusion is, to say the least, doubtful. Moreover, the biaxial (ball-on-three ball) test as such is of doubtful accuracy.

Researchers from TAM Ceramics[49] showed that for their X7P products increasing the number of electrodes within the same part decreases the (three-point bend) strength. Possible explanations for this counter-intuitive result were not discussed. The overall conclusion from their work was that no correlation exists between composition, high firing, low firing, etc., with strength, but also that there is little difference in strength, with the exception of high-density fired dielectrics. They concluded that it is necessary to test each dielectric material individually. Typical strength level for X7R CMCs is 120 MPa.

As far as variation in strength is concerned, only a few data have been reported.[39,50] A value range for the Weibull modulus of about 3–11 has been reported for as-fired CMCs. A typical value is $m = 5$.

As for the dielectric materials as such, a correlation between dielectric breakdown and mechanical breakdown is also observed for CMCs.[51] Rather remarkably these authors also observe an increase in strength when a test voltage is applied. Up to 400 V the strength increases, while at higher voltages a decrease is observed. For this type of test, failure at the end termination was much more frequently observed than for the 0 V strength test. An explanation for these effects was not given.

4.2.3 Subcritical crack growth

The presence of sub-critical crack growth has been mentioned a number of times. Generally this is restricted to qualitative remarks.[46,48] Only limited quantitative data on slow crack growth measured on actual CMCs have been found.[47] In view of the experimental difficulties involved, this is no surprise. For an 'A-type' capacitor sintered with bismuth oxide, under ambient conditions a crack growth exponent $n = 55$ was obtained, while in water the value reduced to $n = 22$. The susceptibility to SCG was attributed to the presence of a Bi-rich phase at the grain boundaries. From these results it seems that the SCG behaviour of the ceramic part of CMCs is similar to that of the monolithic material. Since the fracture path is mainly through the ceramic, this is no surprise. For actual lifetime calculations the effect of residual stress should be considered. The effect on lifetime may be considerable.

4.2.4 Defects

As discussed in Section 2, failure is, apart from the material properties K_{Ic}, etc., also influenced by the presence of defects. Therefore it is useful to know the nature of the defects in CMCs. The following list of defects or defect-generating processes, due to the processing of the CMC itself, can be made:

—Defects due to the separation of the individual CMCs from the laminated plates.
—Burn-out of binder in the dielectric and electrode.[50]
—Green state delaminations, occurring only in dry lamination processes and dependent on the type of binder used.[50]
—Metal–organic catalysis dependent on the metal powder surface area and the presence of coatings.[50]
—Sintering mismatch dependent on Pd content.[50]
—Voids due to air bubbles or binder agglomerates.

The effect of the pick-and-place procedure and further board operations yields defects not directly related to processing of the CMC itself. They include:

—Surface damage due to tumbling.
—Surface damage due to the pick-and-place machines.
—Thermal shock damage due to soldering.

5 Residual stresses

Two types of residual stress can be distinguished. They are related to materials and machining on the one hand and electrodes and terminations on the other hand.

5.1 Residual stresses due to materials and machining

The effect of internal residual stress and surface residual stress on materials has been discussed already in Section 3. Internal residual stress is evidently also of importance for CMCs.

The effect of internal residual stress depends largely upon the grain size of the ceramic used. For materials with a rather small grain size with respect to flaw size, the internal stress averages to zero over the size of the flaw.

Although not reported for CMC materials, it is highly likely that the surface residual stress effect is operating in this case also. Tumbling the fired CMCs, a usual finishing operation, probably introduces similar stresses as during grinding, though possibly of a lower magnitude. The effect of tensile residual stresses above T_C is thus possibly of importance for the soldering procedure. Another aspect of tumbling is the introduction of defects which lower the strength of the material. Some data have been given by Koripella.[39] He describes the change in strength after several cycles in a 'corner rounding apparatus'. A slight increase followed by a small decrease is reported. The Weibull modulus increases by a factor of two initially, but levels out down to about the original value at the end of the process. The strength as a function of tumbling time has been studied in some detail.[53] The strength first decreases due to the introduction of single, larger defects and then increases due to the build-up of residual stress. The final level may be lower or higher than the starting strength level, depending on the precise tumbling conditions.

The only other remarks on surface finish are given by Gee & Stewart.[51] Upon grinding the CMCs with 4000 grit SiC paper, a slight increase in average strength was observed, but the distribution also became much wider. This was explained by the introduction of a few larger flaws lowering the strength values at the low strength side and the introduction of many small flaws increasing the strength at the high strength side of the distribution. The corner rounding procedure and effects involved have been described in some detail.[54] No details on strength have been given, however.

5.2 Residual stresses due to electrodes and terminations

Only a few papers have been published on the internal stress distribution.[47,48] For the case considered (Fig. 6) it has been shown that significant amounts of residual stress can be present. This stress has been determined by indentation techniques. On the free edge, compressive stress with maximum value of 425 MPa is present perpendicular to the free periphery, while tensile stress of magnitude 65 MPa is present parallel to the free periphery. On the end termination edge the behaviour is somewhat complex, but a maximum tensile stress of magnitude 80 MPa is present parallel to the termination, while for the perpendicular direction the tensile stress

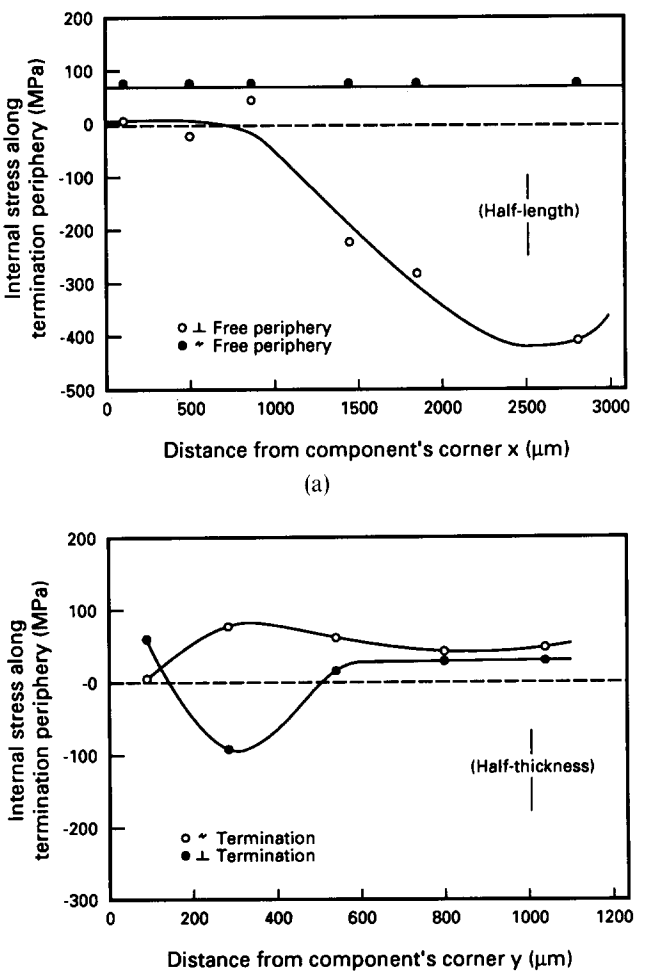

Fig. 6. Residual stress (a) along the free periphery and (b) along the termination side of a CMC. The free periphery is the edge that connects the end terminations, while the termination periphery is the edge covered by the end termination. According to Wong *et al.*[47]

amounts to 40 MPa. The results of Haynes[48] are in agreement with those of Wong *et al.*,[47] although the latter are of a highly qualitative nature.

It has been suggested that the amount of residual stress due to electrodes and terminations can be diminished by undercooling. During undercooling the metal yields further, while upon heating to room temperature some elastic residual stress is left over.[55] For copper it has been estimated that an undercooling of about 50°C is sufficient. While this procedure can be applied to mounted CMCs, it seems likely that the stress situation as generated by undercooling will be destroyed by soldering. Another drawback may be that if extreme care is not taken to avoid capillary condensation, the (anomalous) expansion coefficient of ice may cause significant microcracking, thereby deteriorating the component electrically as well as mechanically.

5.3 Thermal and testing stress

A number of references deal with stress distribution over and in the CMCs during soldering and after mounting. These two aspects will be discussed in the following.

Firstly, let us consider the soldering. It is generally acknowledged[17] that wave soldering yields the severest thermal shock for the CMC followed by vapour phase soldering. Infrared reflow soldering hardly ever shows thermal shock failure. The advantage of decreasing thermal shock susceptibility is compensated by the disadvantage of a decreasing soldering rate. Consequently wave soldering is the technique most often used.

From thermal shock testing the importance of edge effects was stressed.[10] They are said to be the primary source of failure during typical in-service thermal cycling. Consequently it is recommended that the severity of the edge defects could be reduced, but no indication is given on how to reach this goal. Similar general advice has been given by others[11] where the approach of thermal shock testing, fractography and improved processing guided by the fractography was advocated. The severity of edge defects as compared with surface defects was recently discussed in some detail by McCormick.[56]

The stresses during the soldering have been estimated by numerical techniques, notably finite element methods. From these calculations the effect of electrodes has become more clear. While for a monolithic material of 0504 size under certain thermal conditions a transient tensile stress of 24 MPa has been calculated,[57] this reduces to 14 MPa for a CMC with 20 μm dielectric thickness and 1 μm thick Pd electrodes. A further reduction to 10 MPa is present using 2 μm thick electrodes. Other calculations[58,59] show values of tensile stress in the ceramic up to 38 MPa and shear stress in the Sn–Pb layer up to 13 MPa. The latter calculations also indicate that thicker Ni layers in the terminations should yield significantly lower tensile and shear stress, contrary to experimental findings.

A somewhat more detailed discussion was given by Cozzolino.[46] Using a modified plane strain description, the largest stress was found in the ceramic focused under the termination adjacent to the solder pad. A thicker solder pad and a larger fillet height reduced the stress in the ceramic. The largest stresses were found during the soldering and thermal cycling.

These calculations were all of a two-dimensional and elastic nature, but included the temperature–time dependence during soldering.

Contrary to these calculations, Fujikawa *et al.*[60] made (two-dimensional) static elasto-plastic calculations, neglecting the internal electrode structure. These authors indicated a large influence of the introduction of plasticity in the calculations. A difference was made between a small and large amount of solder. A maximum tensile stress of about 20 MPa was observed to be in the transition area between termination and electrode (Fig. 7), in agreement with other results. With the introduction of the soldering, for the top side the tensile stress increased as compared to end termination alone, while in the lower side the orientation was also changed. The maximum stress in the capacitor generated was 30–50 MPa upon applying end termination and soldering. A similar calculation for the stresses in a CMC soldered on a printed circuit, as generated by the bend test (EIA standard RC-3402, glass–epoxy board) with 1, 2 and 3 mm deflection, resulted, however, in much larger stresses.

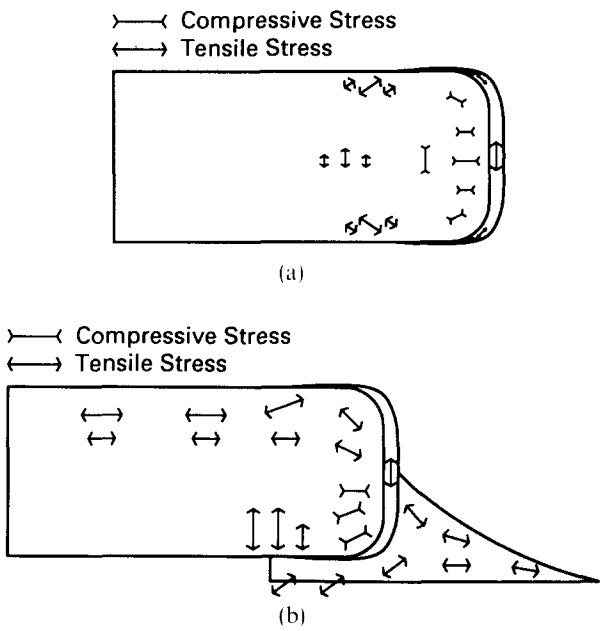

Fig. 7. Stresses in (a) terminated and (b) terminated and soldered CMCs. According to Fujikawa *et al.*[60]

For a 3 mm deflection the stress level ranged from 150 to 200 MPa. Generally for a small amount of solder a somewhat higher stress was calculated, while for a large amount of solder a somewhat lower value was obtained. These values are close to or in excess of the mean failure stress so that most CMCs fail during this test.

Apart from (time-independent) plasticity, time-dependent effects like creep of the metal electrode and end terminations may play a role. This relaxation may lower the compressive residual stress in the ceramic, thereby decreasing the strength. The only reference found is by Freiman. In two of his papers he refers to 'indentation experiments showing no significant change in strength over three orders of magnitude in aging time'. The references (Ref. 23 in Ref. 26 and Ref. 17 in Ref. 30) are actually to a 'to be published paper' which has never appeared as far as could be detected. Provisory long-term indentation experiments in the present author's laboratory showed, however, a steady decrease in hardness with loading time of the indenter.

In summary, one might say that insight is based only on general knowledge of thermal expansion mismatch, elasticity, etc. Optimization and prevention of fracture is sometimes still done using general ideas without detailed modelling.[61] Detailed models of stress distributions are lacking. Calculations made so far are generally of a two-dimensional character. Most workers neglect plasticity effects, while creep and/or relaxation effects have not been addressed at all. In view of the stress level generally reported, a significant relaxation can be expected. Experimental attempts to determine stresses locally are limited and do not yield sufficiently clear answers.

6 Conclusions

The structural integrity of CMCs is a complex field with at least three different subdisciplines related to materials processing, component processing and board processing. Here the author focused on the materials processing.

The most important mechanical parameters of CMC materials and CMCs are the fracture toughness and strength. The toughness of the ceramic in the ferroelectric state (at room temperature) is greater than for the paraelectric state (above the Curie temperature). The strength, however, shows the opposite trend for annealed or as-fired surfaces of fine-grained material. The strength is higher for the paraelectric state. This is attributed to the relief of internal residual stress. For machined surfaces a decrease in strength above the Curie temperature is observed, which is interpreted as originating from a tensile surface residual stress. This stress is due to a different behaviour of machined surfaces as compared with the volume of the material.

As expected, the introduction of electrodes in the material, as in the case of CMCs, increases the fracture toughness and this is thought to be due to the ductility of the metal electrodes. Contrary to the expectation, however, this increase in toughness is not always reflected in a higher strength. The introduction of larger defects in the CMC as compared to the CMC material is probably responsible for this effect.

The variability in strength is large for both the CMC material and the CMCs themselves as reflected by the low Weibull moduli, typically about 5, in various strength measurements. In particular edge defects seem to be particularly detrimental, an effect which has been rationalized recently.

The data on subcritical crack growth show a wide scatter. It is nearly impossible to correlate these data with microstructural information in the absence of the latter. The scarce data suggests that the subcritical crack growth parameters in CMCs are similar to those of the CMC materials. The amount of subcritical crack growth for a specific dielectric ceramic is, however, largely unknown.

It should be stated that only in rare cases sufficient information on the microstructure of the materials involved, necessary for a proper evaluation of the material properties in relation to the microstructure, is provided.

Residual stress due to machining, electrodes and end terminations plays an important role in the mechanical behaviour. The influence of residual stress in the ceramic on the mechanical behaviour of the CMC is, however, inadequately known. Sufficiently realistic theoretical models as well as experimental verifications are lacking. Residual stress may relax by creep and/or relaxation of the yielding parts of the CMC. The effect of relaxation is not known.

All these effects together mean that the material's mechanical behaviour is not directly transferrable to the components. Hence, it must be concluded that there is no overall mechanical model of CMCs which includes plasticity and relaxation of the metal electrodes and end terminations and subcritical crack growth of the ceramic part, while such a model is crucial for the reliable assessment of allowed mechanical loading and longevity.

References

1. Kahn, M., Burks, D. P., Burn, I. & Schulze, W. A., Ceramic capacitor technology. In *Electronic Ceramics*, ed. L. M. Levinson. Marcel Dekker Inc., NY, 1988, pp. 191–274.

2. Hennings, D., Barium titanate based ceramic materials for dielectric use. *Int. J. High Tech. Ceram.*, **3** (1987) 91–111.
3. Day, D. W., High voltage multilayer ceramic capacitors long term stability. In *10th Capacitor and Resistor Technology Symposium CARTS '90*, San Francisco, CA, 1990, pp. 186–9.
4. Waser, R., Bait, T. & Härdtl, K.-H., DC electrical degradation of perovskite type titanates: I. Ceramics. *J. Am. Ceram. Soc.*, **73** (1990) 1645–54. II. Single crystals. *J. Am. Ceram. Soc.*, **73** (1990) 1654–63. III. A model of the mechanism. *J. Am. Ceram. Soc.*, **73** (1990) 1663–74.
5. Boser, O., Kelawon, P. & Geyer, R., Electromechanical resonances in ceramic capacitors and their use for rapid nondestructive testing. *J. Am. Ceram. Soc.*, **72** (1989) 2282–6.
6. Chan, N-H. & Rawal, B. S., An electrically excited acoustic emission test technique for screening multilayer ceramic capacitors. *IEEE Trans. Comp. Hybr. Manuf. Tech.*, **11** (1988) 358–62.
7. Canner, J., Mandai, H. & Wakino, K., The application of acoustic emission to thermal crack detection of multilayer capacitors. In *10th Capacitor and Resistor Technology Symposium CARTS '90*, San Francisco, CA, pp. 24–8.
8. Kish, R., Dietz, K. & Canner, J. P., Use of scanning acoustic microscope for detection of flaws and delaminations in multilayer capacitors. In *Proc. Penn State Multilayer Capacitor Reliability Symp.*, 1989, pp. 153–71.
9. Kessler, L. W. & Semmens, J. E., Characterization of the microstructure of ceramics used in multilayer ceramic capacitors by means of the scanning laser acoustic microscope. *J. Am. Ceram. Soc.*, **72** (1989) 2271–5.
10. Johnson-Walls, D., Drory, M. D., Evans, A. G., Marshall, D. B. & Faber, K. T., Evaluation of reliability of brittle components by thermal stress testing. *J. Am. Ceram. Soc.*, **68** (1985) 363–7.
11. Koripella, C. R. & DeMatos, H. V., Fractography of thermal-shock-cracked multilayer capacitors. *J. Am. Ceram. Soc.*, **72** (1989) 2241–6.
12. Power, III, O. K., Improving thermal shock test reliability. *J. Am. Ceram. Soc.*, **72** (1989) 2264–71.
13. van den Avyle, J. A. & Mecholsky, J. J., Analysis of soldering-induced cracking of $BaTiO_3$ ceramic capacitors. *Ferroelectrics*, **50** (1983) 293–8.
14. Rawal, B. S., Childs, M., Cooper, A. & Mclaughlin, B., Reliability of multilayer capacitors after thermal shock. In *Proc. 38th Elec. Comp. Conf.*, Los Angeles, 1988, pp. 371–5.
15. DeMatos, H. V. & Koripella, C. R., Crack initiation and propagation in MLC chips subjected to thermal stress. In *Proc. CARTS-EUROPE '88*, 1988, pp. 36–42.
16. Marten, G. & Danford, A., Thermal cracking of ceramic capacitors. *CARTS '89 Orlando*, 1989, pp. 31–6.
17. Maxwell, J., Cracks: the hidden defect. In *Proc. 38th Elec. Comp. Conf.*, Los Angeles, 1988, pp. 376–84.
18. Davidge, R. W., *Mechanical Behaviour of Ceramics*. Cambridge Univ. Press, 1979.
19. Lawn, B. R. & Wilshaw, T. R., *Fracture of Brittle Materials*. Cambridge Univ. Press, 1975.
20. Suo, Z., Kuo, C.-M., Barnett, D. M., Willis, J. R., Fracture mechanics for piezoelectrical ceramics, *J. Mech. Phys. Solids*, **40** (1992) 739–65.
21. Pohanka, R. C., Smith, P. L. & Pasternak, J., The static and dynamic strength of piezoelectric materials. *Ferroelectrics*, **50** (1983) 285–91.
22. Pohanka, R. C., Freiman, S. W., Okazaki, K. & Tashiro, S., Fracture of piezoelectric materials. In *Fracture Mechanics of Ceramics*, Vol. 5, ed. R. C. Bradt, A. G. Evans, D. P. H. Hasselman & F. F. Lange. Plenum Press, NY, 1983, pp. 353–64.
23. Pohanka, R. C., Rice, R. W. & Walker, Jr, B. E., Effect of internal stress on the strength of $BaTiO_3$. *J. Am. Ceram. Soc.*, **59** (1976) 71–4.
24. Pohanka, R. C., Rice, R. W., Walker, B. E. & Smith, P. L., Fracture, fractography and internal stress of $BaTiO_3$ ceramics. *Ferroelectrics*, **10** (1976) 231–5.
25. Baker, T. L. & Freiman, S. W., Fracture behaviour of ceramics used in multilayer capacitors. In *Electronic Packaging Materials Science II*, ed. K. A. Jackson, R. C. Pohanka, D. R. Uhlmann & D. R. Ulrich. *Mater. Res. Soc. Symp.*, **72** (1986) 81–90.
26. Freiman, S. W., Fracture behaviour of electronic ceramics. *Ferroelectrics*, **102** (1990) 381–90.
27. Pohanka, R. C., Freiman, S. W. & Bender, B. A., Effect of phase transformation on the fracture behaviour of $BaTiO_3$. *J. Am. Ceram. Soc.*, **61** (1978) 72–5.
28. Pohanka, R. C., Freiman, S. W. & Rice, R. W., Fracture processes in ferroic materials. *Ferroelectrics*, **28** (1980) 337–42.
29. Cook, R. F., Freiman, S. W., Lawn, B. R. & Pohanka, R. C., Fracture of ferroelectric ceramics. *Ferroelectrics*, **50** (1983) 267–72.
30. Freiman, S. W. & Pohanka, R. C., Review of mechanically related failures of ceramic capacitors and capacitor materials. *J. Am. Ceram. Soc.*, **72** (1989) 2258–63.
31. de With, G. & Parren, J. E. D., Surface stresses in modified $BaTiO_3$ ceramics. *Brit. Ceram. Soc. Proc.*, **34** (1984) 99–108.
32. Arlt, G., Twinning in ferroelectric and ferroelastic ceramics: stress relief. *J. Mater. Sci.*, **25** (1990) 2655–66.
33. Buessem, W. R., Cross, L. E. & Goswami, A. K., Phenomenological theory of high permittivity in fine-grained barium titanate. *J. Am. Ceram. Soc.*, **49** (1966) 33–6.
34. Cozzolino, M. J. & Ewell, G. J., A fracture mechanics approach to structural reliability of ceramic capacitors. *IEEE Trans. Comp. Hybr. Manuf. Tech.*, **3** (1980) 250–7.
35. Pisarenko, G. G., Chushko, V. M. & Kovalev, S. P., Anisotropy of fracture toughness of piezoelectric ceramics. *J. Am. Ceram. Soc.*, **68** (1985) 259–65.
36. Grekov, A. A. & Kramarov, S. O., Mechanical strength of ferroelectric ceramics. *Ferroelectrics*, **18** (1978) 249–55.
37. Ewell, G. J., Critical mechanical properties of ceramic chip capacitors. *Proc. CARTS-EUROPE '88*, 1988, pp. 60–70.
38. McKinney, K. R., Rice, R. W. & Wu, C. M., Mechanical failure characteristics of ceramic multilayer capacitors. *J. Am. Ceram. Soc.*, **69** (1986) C228–C223.
39. Koripella, C. R., Mechanical behaviour of ceramic capacitors. *IEEE Trans. Comp. Hybr. Manuf. Tech.*, **14** (1991) 718–24.
40. Yamashita, K., Koumoto, K. & Yanagida, H., Analogy between mechanical and dielectric strength distributions for $BaTiO_3$ ceramics. *J. Am. Ceram. Soc.*, **67** (1984) C11–C13.
41. Kishimoto, A., Koumoto, K. & Yanagida, H., Mechanical and dielectric failure of $BaTiO_3$ ceramics. *J. Mater. Sci.*, **24** (1989) 698–702.
42. Kishimoto, A., Koumoto, K., Yanagida, H. & Nameki, M., Microstructure dependence of mechanical and dielectric strength. I. Porosity. *Eng. Fract. Mech.*, **40** (1991) 927–30.
43. McHenry, K. D. & Koepke, B. G., Mechanical reliability of Z5U capacitors. In *Electronic Packaging Materials Science II*, ed. K. A. Jackson, R. C. Pohanka, D. R. Uhlmann & D. R. Ulrich. *Mater. Res. Soc. Symp.*, **72** (1986) 113–19.
44. de With, G. & Parren, J. E. D., Fracture of modified $BaTiO_3$ ceramics. *Silicates Industriels*, **9** (1984) 179–83.
45. Fuller, E. R., Lawn, B. R. & Cook, R. F., Theory of fatigue for brittle flaws originating from residual stress concentrations. *J. Am. Ceram. Soc.*, **66** (1983) 314–21.
46. Cozzolino, M. J., Stress determination for surface mounted ceramic capacitors. In *Proc. CARTS '86*, 1986, pp. 42–52.
47. Wong, B., Holbrook, R. J., Megerle, C. A. & Medina, L. E., Microindentation for mechanical assessment of microelectronic components. In *Proc. 1986 Int. Symp. Microelectronics*, Int. Soc. Hybrid Microelectron., Reston, VA, 1986, pp. 399–410.
48. Haynes, R., Cracking of surface mount capacitors: crack susceptibility by Vickers indentation techniques. *J. Am. Ceram. Soc.*, **72** (1989) 2292–4.
49. Pollock, K. L. & Hodgkins, C. E., Fracture strength of multilayer ceramic capacitors. In *Proc. 1984 Symp. Microelectronics*, Int. Soc. Hybrid. Microelectron., Montgomery, AL, 1984, pp. 450–6.

50. Morrell, R. & Gee, M. G., Mechanical testing of MLCC's. In *Proc. 2nd Eur. Conf. Adv. Mater. (Euromat '91), Inst. Materials*, **3** (1992) 13–28.
51. Gee, M. G. & Stewart, M., Electromechanical testing of multilayer ceramic capacitors. *CARTS Europe* (1992) 151–166.
52. Pepin, J. G., Borland, W., O'Callaghan, P. & Young, R. J. S., Electrode-based causes of delaminations in multilayer ceramic capacitors. *J. Am. Ceram. Soc.*, **72** (1989) 2287–91.
53. de With, G. & Sweegers, N., Strength of and residual stress in ceramic multilayer capacitors after tumbling. *J. Eur. Ceram. Soc.*, in preparation.
54. Chen, S. K., Chang, C. P. & Liu, H. S., Aspects of erosional wear during tumbling of $BaTiO_3$ dielectric ceramics. *Wear*, **147** (1991) 345–53.
55. Hsueh, C. M. & Evans, A. G., Residual stresses in metal/ceramic bonded strips. *J. Am. Ceram. Soc.*, **68** (1985) 241–8.
56. McCormick, N. J., The edge flaking of brittle materials. *Brit. Ceram. Proc.*, **46** (1990) 307–18.
57. Canner, J. P., Toda, K., Okada, T. & Wakino, K., The analysis of thermal stress in monolithic capacitors using finite element method. In *Proc. Penn State Multilayer Capacitor Reliability Symp.*, 1989, pp. 219–29.
58. Scott, G. C. & Astfalk, G., Modeling thermal stress behavior in microelectronic components. *Trans. ASME, J. Electr. Packag.*, **112** (1990) 35–40.
59. Scott, G. C. & Astfalk, G., A model of thermal stress development in microelectronic components. In *Electronic Packaging Materials Science IV*, ed. R. Jaccodine, K. A. Jackson, E. D. Lillie & R. C. Sundahl. *Mater. Res. Soc. Symp.*, **154** (1990) 473–8.
60. Fujikawa, N., Inagaki, M. & Yokue, N., Simulation and evaluation of stresses in surface mounted chip capacitors. *Ceram. Trans.*, **8** (1990) 292–302.
61. Martel, M., The case of cracked caps. *Circuits Manuf.*, **8** (1987) 55–7.